HHS Public Access

Author manuscript

Congenit Heart Dis. Author manuscript; available in PMC 2018 May 01.

Published in final edited form as:

Congenit Heart Dis. 2017 May ; 12(3): 322–331. doi:10.1111/chd.12443.

Increased Regurgitant Flow Causes Endocardial Cushion Defects in an Avian Embryonic Model of Congenital Heart Disease

Stephanie M Ford, MD[1], **Matthew T McPheeters, MS**[3], **Yves T Wang, PhD**[4], **Pei Ma, PhD**[4], **Shi Gu, PhD**[4], **James Strainic, MD**[2], **Christopher Snyder, MD**[2], **Andrew M Rollins, PhD**[4], **Michiko Watanabe, PhD**[3], and **Michael W Jenkins, PhD**[3]

[1]University Hospitals, Rainbow Babies and Children's Hospital Division of Neonatology, Cleveland, OH

[2]University Hospitals, Rainbow Babies and Children's Hospital Division of Pediatric Cardiology, Cleveland, OH

[3]Case Western Reserve University School of Medicine, Department of Pediatric Cardiology, Cleveland, OH

[4]Case Western Reserve University Department of Biomedical Engineering, Cleveland, OH

Abstract

Background—The relationship between changes in endocardial cushion and resultant congenital heart diseases (CHD) has yet to be established. It has been shown that increased regurgitant flow early in embryonic heart development leads to endocardial cushion defects, but it remains unclear how abnormal endocardial cushions during the looping stages might affect the fully septated heart. The goal of this study was to reproducibly alter blood flow *in vivo* and then quantify the resultant effects on morphology of endocardial cushions in the looping heart and on CHDs in the septated heart.

Methods—Optical pacing was applied to create regurgitant flow in embryonic hearts, and optical coherence tomography (OCT) was utilized to quantify regurgitation and morphology. Embryonic quail hearts were optically paced at 3 Hz (180bpm, well above intrinsic rate 60–110bpm) at stage

Corresponding author: Stephanie Ford, University Hospitals, 11100 Euclid Ave, MS 6010, Cleveland, OH 44106, Phone: (216) 844-3387, Fax: (216) 844-3380, Stephanie.ford@uhhospitals.org.

Authors have no disclosures or conflicts of interest

Author Contributions:

Stephanie M Ford, MD: concept/design, data collection, data analysis and interpretation, drafting article, critical revision of article, approval of article, secured funding

Matthew T McPheeters: data collection, data analysis and interpretation, critical revision of article, approval of article

Yves T Wang, PhD: data collection, data analysis and interpretation, critical revision of article, approval of article

Pei Ma, PhD: concept/design, critical revision of article, approval of article

Shi Gu, PhD: data analysis/interpretation, statistical analysis, critical revision of article, approval of article

James Strainic, MD: data analysis/interpretation, critical revision of article, approval of article

Christopher Snyder, MD: data analysis/interpretation, critical revision of article, approval of article

Andrew M Rollins, PhD: data analysis/interpretation, critical revision of article, approval of article, secured funding

Michiko Watanabe, PhD: concept/design, data analysis/interpretation, critical revision of article, approval of article, secured funding

Michael W Jenkins, PhD: concept/design, data analysis and interpretation, statistical analysis, drafting article, critical revision of article, approval of article, secured funding

13 of development (3–4 wks human) for 5 min. Pacing fatigued the heart and led to at least 1 hr of increased regurgitant flow. Resultant morphological changes were quantified with OCT imaging at stage 19 (cardiac looping – 4–5 wks human) or stage 35 (4 chambered heart – 8 wks human).

Results—All paced embryos imaged at stage 19 displayed structural changes in cardiac cushions. The amount of regurgitant flow immediately after pacing was inversely correlated with cardiac cushion size 24-hrs post pacing (p-value < 0.01). The embryos with the most regurgitant flow and smallest cushions after pacing had a decreased survival rate at 8 days ($p<0.05$), indicating that those most severe endocardial cushion defects were lethal. Of the embryos that survived to stage 35, 17/18 exhibited CHDs including valve defects, ventricular septal defects, hypoplastic ventricles, and common AV canal.

Conclusion—The data illustrate a strong inverse relationship in which regurgitant flow precedes abnormal and smaller cardiac cushions, resulting in the development of CHDs.

Keywords

Endocardial Cushion Defect; Regurgitant Flow; Optical Coherence Tomography; Optical Pacing; Optical Control

Introduction

The mechanisms leading to the development of congenital heart diseases (CHDs) remain largely unclear. Only a minority of CHDs can be traced to a specific agent such as maternal metabolic disease, diabetes, or exposure to organic solvents or therapeutic drugs.[1] Both genetic and environmental factors have been implicated as causes of CHDs. The genetic factors contributing to CHDs range from single gene mutations to complex chromosomal rearrangements.[2,3] However, genetic mutations yield widely varying phenotypes in affected individuals and lead to a large variety of malformations. The expression of environmentally-induced CHDs, including maternal exposure to alcohol,[4–6] drugs,[7] hypoxia,[8,9] and viral infections[1,10] also present quite differently from individual to individual. In addition, many common CHDs can be triggered by a genetic mutation or environmental factor.[1,11] These facts suggest that CHDs may be caused by the complex interplay between genetics and environment.

The intersection of genetic and environmental forces in the etiology of CHDs may lie in the simplistic concept of how they alter blood flow. This theory of alterations in blood flow leading to CHDs was first proposed in the 1970s by Fishman et al.[12] This study demonstrated that restricting blood flow to the left ventricle in fetal lambs, resulting from either left ventricular inflow or outflow tract obstruction, gives rise to hypoplastic left heart syndrome.[12] Other studies demonstrated that the fetal ventricle is sensitive to afterload, such that small changes in aortic pressure or afterload have negative effects on left ventricular stroke volume.[13] Changes in afterload in the fetal ventricle also led to decreased blood flow through the left ventricle, resulting in hypoplasia.[13]

Recently, studies have demonstrated that abnormal fetal blood flow through the developing heart can affect cardiac formation much earlier in development.[14–28] For example vitelline vein ligation in avian embryos at looping stages altered blood flow in the tubular outflow

tract and induced ventricular septal defects, semilunar valve anomalies, and pharyngeal arch artery malformations.[18] Other studies have applied conotruncal banding and atrial ligation to establish the connection between early blood flow and fetal cardiac formation.[14,17–19,24,26–28] These hemodynamic forces may exert their effects on heart development through regulation of mechanosensitive gene and protein expression (e.g., KLF2), which forms a feedback loop by influencing resultant cardiac structure and hemodynamics.[17,20–24] Despite these new findings, limited information exists as to how, when, and to what degree the developing cardiovascular system is most vulnerable to abnormal cardiac function. Establishing the causality between abnormal embryologic hemodynamics and CHDs requires improved tools for both perturbing and monitoring *in vivo* embryos.

Previous methods to perturb fetal hemodynamics (e.g., conotruncal banding,[16,24,26,27,29] vessel ligation[14,17,18]) lacked precision as well as repeatability, and they caused gross, non-physiologic hemodynamic changes. Unfortunately, electrical pacing, a common tool to study cardiac dynamics, is invasive when applied to the early looping heart (e.g., requires direct contact with the heart which may damage these delicate tissues). It has therefore not been employed as a perturbation tool. One alternative to surgical or obstructive methods for controlling hemodynamics in live embryos is optical pacing (OP). The technique of using infrared light to stimulate compound action potentials was pioneered in nerves.[30] OP is a similar method that utilizes pulsed infrared light directed on the myocardium to initiate cardiac contraction. Jenkins *et al.* demonstrated reliable cardiac OP in quail embryos over a range of developmental stages without producing signs of damage to the tissue.[31] Since this initial report, OP has been demonstrated in a variety of animal models.[32,33] The specific mechanisms for OP to cause cardiac conduction has yet to be defined, but an induced thermal gradient appears to produce the desired effect.[34] Both altered membrane capacitance[35] and mitochondrial calcium transients[36] have also been implicated as causes. OP has the potential to overcome the limitations of previous perturbation techniques because it is noninvasive, repeatable, precise, and can mimic hemodynamic anomalies present in CHDs.

In this experiment, OP increased regurgitation in the embryonic quail heart at stage 14 (looping heart prior to the development of cardiac cushions), while optical coherence tomography (OCT) measured the level of regurgitation and the resultant heart morphology at stage 19 (looping heart with cardiac cushions) and 34 (four-chambered heart). Paced hearts reliably developed common CHDs (e.g., Ebstein's Anomaly, Common Atrioventricular Canal, etc.) at stage 34 consistent with endocardial cushion defects. These studies reveal a precise relationship between regurgitant flow, endocardial cushion volume, and CHDs in a reliable *in vivo* model. These data suggests that increased regurgitant flow in the looping quail heart leads to smaller endocardial cushions that result in CHDs.

Methods

Avian Model

IACUC approval was not required for this study, which involves the utilization of avian embryos that were collected at embryonic day 8 at the latest.

Fertilized quail eggs (Coturnix coturnix communis; Boyd's Bird Company, Inc., Pullman, WA) were incubated in a humidified incubator (G.Q.F. Manufacturing Co., Savannah, GA) at 37°C. At stage 14,[37] the eggs were taken from the incubator, the eggshell removed, and the contents placed in a 3.5cm Petri dish. Embryos were then housed in an incubator until completion of the study.

Optical Pacing (OP)

A diode laser (Capella; Lockheed Martin Aculight, Bothell, WA) centered at 1860 nm was employed to pace day 2 quail hearts. Laser light was coupled into a 600 μm multimode fiber with an aspheric lens at the tip. The fiber was placed on a micromanipulator and positioned so an 800 μm (full-width half-maximum (FWHM)) spot illuminated in inflow portion of the heart tube. Hearts were stimulated with 10 ms pulses at 3.0 Hz for 5 minutes with a radiant exposure of 0.63–1.38 J/cm^2 per pulse. Laser energy was measured with a pyroelectric energy meter (Ophir, North Andover, MA). Radiant exposures per pulse were calculated by dividing the measured pulse energy by the spot size area at the tissue surface. The temperature increase due the laser was measured with a thermal camera (A325; Flir, Wilsonville, OR). A maximum temperature increase of 4° C was measured at the tissue surface, which indicates a lower temperature maximum at the heart several hundred microns below the surface.

Optical Coherence Tomography (OCT)

OCT achieves range-gated sub-surface microscopic imaging of biological samples by use of low-coherence interferometry.[38] It has high spatial resolution (2–20 μm), high temporal resolution (> 100 kHz line rates), deep optical penetration (1–3 mm in embryonic tissues), and Doppler flow sensing.[39–41] A custom-built spectral domain OCT system[42] was utilized for the experiments in this study. The OCT light source has a center wavelength at 1310 nm and a FWHM bandwidth of 75 nm leading to an axial resolution of ~10 μm in air. This system utilized a linear-in-wavenumber spectrometer as previously described.[42] The line scan camera (Sensors Unlimited, Princeton, NH) in the OCT spectrometer read out lines at 47 kHz. A compact scanner placed in a commercial incubator (Galaxy 170R; Eppendorf, Hamburg, Germany) was employed to image the embryo during and after OP and had a lateral resolution of 32 μm (See Figure 1). The incubator kept the temperature at 37 °C and the humidity at approximately 80%. Three linear actuators (Zaber, Vancouver, British Columbia) controlled with software (LabVIEW; National Instruments, Austin, TX) allowed positioning of each egg from outside the incubator. A less compact scanner with higher lateral resolution (10 μm) imaged fixed embryonic hearts at day 3 and 8.

Experimental Methods

Pacing Experiments Stage 14—Quail embryos were cracked into shell-less cultures and placed into our incubator equipped with OP and OCT. The pacing laser was focused on the inflow tract of the heart. Embryos were paced at 180 beats per minute (bpm), or 3Hz, for 5 minutes. The intrinsic heart rate at this stage is 60–110bpm. Heart rate was confirmed in real-time with 2-D OCT images and a metronome. OCT pulsed Doppler traces (near the atrioventricular junction) and 2-D structural images were collected before, during,

immediately after, and one hour after pacing. See Figure 2 for timeline. To control for effects of light or temperature aside from the rapid pacing, a subset of embryos (n=7) were paced 10 bpm above their intrinsic rate and their cushion volumes were compared to other controls and paced embryos. To control for temperature increases induced by the laser, a subset of embryos (n=9) at stage 14 were placed in an incubator preheated to 43 °C for 90 minutes before being returned to an incubator at 37 °C until stage 19. The maximum increase in temperature induced by the laser was 4 °C, which is a lower temperature increase than that exposed to the controls. Another set (n=7) of control embryos were cracked into shell-less cultures at stage 14 and allowed to grow without further intervention.

Cushion Assessment stage 19 (day 3)—Cushion volumes were assessed for all paced (n=8) and control embryos (n=23) at stage 19. Embryos were fixed in formalin and then washed in PBS three times for 5 minutes. All hearts were dissected from the body and imaged with OCT at completion of the experiment. Raw imaging data was processed with Matlab (The MathWorks, Natick, Massachusetts) and analyzed with Amira (Visage Imaging GmbH, Berlin, Germany). Each heart was manually segmented to calculate total volume of the endocardial cushions. The same investigator segmented all hearts for consistency.

Congenital Heart Defect Assessment stage 34 (day 8)—After pacing at stage 14, embryos were allowed to mature in shell-less cultures in the incubator. Each embryo was checked at least once daily to monitor viability. Those embryos surviving to day 8 were sacrificed, and the hearts dissected. A subset of embryos (n=7) were left in the egg until day 8 and employed as controls. All hearts were relaxed in 0.5M KCL and fixed in formalin. Hearts were then optically cleared using ClearT as previously described.[43,44] Each heart was imaged with OCT, and the raw data converted to image files with Matlab and visualized with Amira. All heart images, control and paced, were given in a blinded fashion to a Pediatric Cardiologist with expertise in fetal echocardiographic interpretation for review.

Statistical analyses were performed in Minitab 17 (Minitab Inc., State College, PA). Comparisons of cardiac cushion volumes for the control and paced populations were performed using one-way ANOVA, and post-hoc comparisons were performed with Tukey's method using a 90% confidence interval. The relationship between cardiac cushion volume and regurgitant flow percentage after pacing was assessed using a linear regression. The percentages of regurgitant flow after pacing for dead and living embryo populations at day 8 were compared using a Student's *t*-test with a 95% confidence interval.

Results

We first examined how an interval of rapid OP alters blood flow patterns in the embryonic quail heart at day 2 (stage 14) of development. Figure 3 illustrates pulsed Doppler OCT traces captured in the inflow region, during, immediately after, and one hour following OP in a serial study of a representative embryo. Tracings before and during pacing show a normal, minor amount of regurgitant flow. Immediately after pacing there is a large amount of regurgitant blood flow, which is a common finding when the heart is paced well above its intrinsic rate. One hour after pacing, the forward flow in the heart has recovered, yet a large

amount of regurgitant flow remains. Increased regurgitation lasted for at least an hour after pacing ceased in all paced embryos.

The heart volumes were imaged with OCT 24 hours after pacing was performed. Figure 4 illustrates the 2-D slices of a control and paced heart on day 3 (stage 19). The control heart maintains a normal atria (A), ventricle (V) and outflow tract (OFT). In the control heart, the AV cushions are appropriately sized, and contain many endothelial mesenchymal transition (EMT) cells indicated by the bright speckles within the cushions. The EMT cells are the stem cells responsible for valve and OFT formation. The paced heart clearly illustrates an abnormally shaped and oriented OFT. The AV cushions (arrows) appear smaller than the control, they do not abut each other, and they contain regions of increased and decreased mesenchymal cells. The gap between the AV cushions makes it impossible for them to properly function and occlude regurgitant blood flow. The cushions in the OFT are similarly small and almost devoid of EMT.

Figure 5A demonstrates that cardiac cushion volumes on day 3 (stage 19) were lower in the cohort of embryos paced well above the intrinsic rate on day 2 (stage 14) compared with controls. Controls included untreated embryos, embryos exposed to 43 °C for 90 minutes instead of pacing, and embryos paced slightly above their intrinsic rate. A two-way ANOVA with a post-hoc Tukey test determined that the paced embryos had a statistically significant difference in volume compared to the controls, both as individual groups and as a whole. None of the controls were statistically different from each other. We also found a direct correlation ($p<0.01$) between the regurgitant flow fraction one hour after pacing and endocardial cushion volume a day later (Figure 5B). Control fetal heats had a mean cushion volume of $0.161mm^3 \pm 0.029mm^3$, whereas paced fetal hearts had a mean volume of $0.103 mm^3 \pm 0.059mm^3$, $p<0.05$. If the OP hearts are split between those with low regurgitant flow and those with high, the disparities become more pronounced; $0.150 mm^3 \pm 0.022mm^3$ vs $0.056 mm^3 \pm 0.044mm^3$ respectively. For comparison, controls had regurgitant flow under 5%. To determine how these abnormal cushions would affect further development, embryos were paced and allowed to mature to day 8 (stage 34), when the quail heart is fully septated. The embryos with the largest regurgitant flow fraction, which correlated to the smallest endocardial cushions, had a high mortality rate between days 4 and 8 (Figure 6). The reduced cushion volumes indicate that hemodynamic changes can influence structure formation even after the insult has been withdrawn.

Paced embryos that survived to day 8 were imaged with OCT. To enable imaging through the entire heart, the hearts were optically cleared.[43,44] All images of the hearts were interpreted by an expert echocardiographer. All 7 controls were identified as normal, while only one paced embryo was considered normal. Figure 7 shows a control and several examples of paced embryos with CHDs. Table 1 displays the defects observed in all day 8 hearts that were paced. One paced embryo died just before day 8, but was intact and suitable to be imaged for analysis. Of the 18 hearts that survived to be imaged on day 8, 17 had at least one defect and many were found to have more than one defect. The majority of defects identified have been previously linked to endocardial cushion defects. These hearts were all within the lower end of increased regurgitant flow seen in Figure 5b, but still displayed

easily recognizable and clinically significant heart defects. This finding suggests that even slight increases in regurgitant flow may contribute to the formation of CHDs.

Discussion

In this study, we have demonstrated altered hemodynamics in wild-type avian embryos, through increased regurgitant flow, proceeds and likely leads to decreased endocardial cushion size and clinically relevant CHDs. It has been previously published that retrograde flow acts as an important factor for endocardial cushion development[45]. Due to the fact that endocardial cushions form the AV valves and some of the atrial and ventricular septa in the mature heart, numerous CHDs may originate from abnormal formation of these cardiac cushions. To understand the relationship between regurgitant flow and CHDs, we must be able to accurately and precisely perturb blood flow, quantify the hemodynamics, and then measure the structural and genetic downstream effects. Inducing hemodynamic abnormalities have previously been accomplished with atrial ligation, vitelline vessel ligation, bead obstruction, and conotruncal banding.[14,16–18,24,26–28] These studies revealed that altered blood flow in early development yields cardiac defects. In 2009, Vermot *et al.* demonstrated that changes in regurgitant flow act through KLF2 expression to alter valve development in zebrafish embryos.[19] Other papers have verified ties between regurgitant flow and altered expression of genes, such as KLF2, NOS3, rhoA, and NFKB.[24,46,47] Regurgitant flow has also been implicated as a contributing factor to human disease models, such as those defects associated with prenatal alcohol exposure. Karunami *et al.* observed that embryonic ethanol exposure in an avian model induced increased regurgitant flow in vitelline vessels that preceded valve and septal defects.[4]

Each of these studies examines a piece of the puzzle, from creating hemodynamic changes, to observing the regurgitant blood flow or shear stress, to the resulting CHDs. However, none of these studies were able to investigate all areas with a cohesive model, nor could they quantify the regurgitant flow and cushion defects. We built on this work by using more precise hemodynamic monitoring techniques, and quantifying cushion formation, and following the embryos to fully formed 4-chambered hearts. We have also demonstrated a new perturbation technology (OP) which might overcome some of the previous limitations, which involved structural and non-physiologic changes. With the unique combination of OP and OCT imaging, we can now quantify functional and morphological measurements in stages ranging from the tubular to the 4-chambered heart. Furthermore, these results confirm a strong correlation between regurgitant flow in the tubular heart, abnormal endocardial cushion development, and clinically significant cardiac defects.

As OP is a newer method that can be utilized for controlling hemodynamics, we were careful to include experiments that would exclude components of the pacing itself as causes for defects. The temperature controls confirm that it is not the increased temperature that causes changes to the endocardial cushions. The controls paced slightly above their intrinsic rate likewise demonstrate that the light or pacing itself do not cause changes to the endocardial cushions. Furthermore, the amount of increased regurgitant flow is strongly correlated to decreasing endocardial cushion size and congenital heart defects. There may be

additional forces at work contributing to these changes, such as altered myocardial contractility, but the full extent of this contribution could not be ascertained in this study.

It is important to establish that our pacing-induced defects are physiological relevant. Here, we show the similarities of pacing-induced defects with our prenatal alcohol exposure and cardiac neural crest cell ablation models (see Figure 8).[4,48] The first column shows controls; the second, embryos exposed to ethanol during gastrulation (prenatal alcohol exposure model); the third, embryos whose cardiac neural crest cells were ablated; and the fourth, embryos that were optically paced. A–D are representative day 3 3-D OCT reconstructions. The ethanol-exposed (B), CNCC-ablated (C), and optically paced (D) body morphologies all commonly display abnormal spinal curvature. This is fascinating considering that CHDs are strongly associated with scoliosis.[49,50] Each of these experimental models has increased regurgitant flow, abnormal endocardial cushions, and CHDs at the 4-chamber stage. We believe altered hemodynamics is a contributing factor in all three models, which may explain the similar phenotypes. These similarities among disparate models suggest that regardless of the initial insult, an increase in regurgitant flow results in abnormal endocardial cushions and later CHDs. Furthermore, this suggests that CHDs may have a common cause. This may also explain why those with identical genetic abnormalities have diverse CHD phenotypes, as different amounts of regurgitant flow would lead to separate morphologies.

The clinical implications of this model are significant. Approximately 7.5% of all live births in the US have some form of CHD (including BAV and all VSDs that spontaneously close), but only 0.6–0.7% are moderate to severe CHDs.[51,52] Worldwide, this equates to 1.35 million live births with CHD every year,[53] representing a substantial and costly health problem. While VSDs are the most common CHD and a common defect in this study, what is additionally interesting is the trend toward right–sided heart lesions. These include pulmonary valve dysplasia and stenosis, tricuspid valve abnormalities (dysplasia to Ebsteinoid), and right ventricular hypertrophy or dilatation. These diseases have an incidence of 1.3 live births per 1000,[51] but include significant morbidity throughout life including valve replacement, multi-step palliative procedures, and arrhythmia control. Here, we have created a reliable animal model of these defects, which is the first step in ultimately finding possible interventions or methods of prevention.

Currently, of those patients presenting with CHD, only about 8–12% will have an identified genetic aberration.[54,55] Furthermore, identical mutations known to cause CHDs cause a variety of phenotypes. This indicates there must be a more intricate explanation for the formation of CHDs than simply genetics. A feedback loop involving shear stress and abnormal blood flow, genetic expression, and cushion formation ties together the current known information on early CHD phenotypes. This integrated model highlights the importance of function in the foundation of CHDs, regardless of which environmental or genetic inciting factors are involved. Understanding the interplay between these factors is critical to identifying the origin of CHDs.

This combined OP and OCT system has proved to be a reliable method for exploring effects of regurgitant flow on CHD. However, there are drawbacks to this design. Light-tissue interactions are complex, and though the controls and experimental design were created to

limit known variables, it is impossible to exclude all other facets of these interactions as causal to these results. The intent of pacing is to increase the heart rate, and other physical forces, such as myocardial stretch and depleted energy stored in the myocytes, may be contributing to these results. The largest limitation is inherent to the OCT imaging system. OCT has a penetration depth of only a few millimeters. Therefore this type of imaging with its current technological restraints cannot be used in a placental animal model.

How these forces change genetic expression in real time is still mostly unknown. To tie together the abnormal function of the heart and the changes in endocardial cushions, it will be crucial to examine how these developmental pathways are transduced, how those pathways are altered, and in which ways this changes RNA expression. Future experiments should be directed toward how modified molecular expression may feedback to cause further functional changes. Another powerful tool that explores these interactions is 4-D shear stress mapping. Peterson *et al and* others have shown 4-D shear stress maps are possible.[40,56] Combining this information with the 3-D expression of genetic markers would considerably expand our understanding of the pathogenesis of CHDs.

Conclusion

We have noninvasively increased regurgitant flow *in vivo* in tubular hearts in a consistent quantifiable fashion, and the amount of regurgitant flow inversely correlates with the subsequent formation of abnormal endocardial cushions. These abnormal endocardial cushions then lead to clinically relevant CHDs in a 4-chambered avian model. Moreover, increased regurgitant flow is common among multiple disease models, indicating that it may be an underlying pathology for CHDs.

Acknowledgments

Grants and funding:

National Institutes of Health R21-HL115373, R21-HL123012, R01-HL126747, RO1-HL095717.

The University Hospitals Rainbow Foundation

The Marshall Klaus Perinatal Research Award

Thank you to Matthew R Ford, PhD, for his generous assistance with Matlab coding and data processing.

References

1. Jenkins KJ, Correa A, Feinstein JA, et al. Noninherited Risk Factors and Congenital Cardiovascular Defects: Current Knowledge: A Scientific Statement From the American Heart Association Council on Cardiovascular Disease in the Young: Endorsed by the American Academy of Pediatrics. Circulation. 2007; 115(23):2995–3014. DOI: 10.1161/CIRCULATIONAHA.106.183216 [PubMed: 17519397]
2. Cowan JR, Ware SM. Genetics and Genetic Testing in Congenital Heart Disease. Clin Pernatol. 2015; 42(2):373–393. DOI: 10.1016/j.clp.2015.02.009
3. Mitchell ME, Sander TL, Klinkner DB, Tomita-Mitchell A. The Molecular Basis of Congenital Heart Disease. Semin Thorac Cardiovasc Surg. 2007; 19(3):228–237. DOI: 10.1053/j.semtcvs.2007.07.013 [PubMed: 17983950]

4. Karunamuni G, Gu S, Doughman YQ, et al. Ethanol exposure alters early cardiac function in the looping heart: a mechanism for congenital heart defects? Am J Physiol Heart Circ Physiol. 2014; 306(3):H414–H421. DOI: 10.1152/ajpheart.00600.2013 [PubMed: 24271490]
5. Serrano M, Han M, Brinez P, Linask KK. Fetal alcohol syndrome: cardiac birth defects in mice and prevention with folate. YMOB. 203:75.e7–e75.e15. DOI: 10.1016/j.ajog.2010.03.017
6. Steeg CNP, Woolf N, York NY. Cardiovascular malformations in the fetal alcohol syndrome. Am Heart J. 1979; 98(5):635–7. [PubMed: 158960]
7. Tintu, A., Rouwet, E., Verlohren, S., et al. Hypoxia Induces Dilated Cardiomyopathy in the Chick Embryo: Mechanism, Intervention, and Long-Term Consequences. In: Schwartz, A., editor. PLoS One. Vol. 4. 2009. p. e5155
8. Neill CA. Etiology of congenital heart disease. Cardiovasc Clin. 1972; 4(3):137–147. [PubMed: 4591014]
9. Wikenheiser J, Wolfram JA, Gargesha M, et al. Altered Hypoxia-inducible factor-1 alpha expression levels correlate with coronary vessel anomalies. Dev Dyn. 2009; 238(10):2688–2700. DOI: 10.1002/dvdy.22089 [PubMed: 19777592]
10. Oster ME, Riehle-Colarusso T, Correa A. An update on cardiovascular malformations in congenital rubella syndrome. Birth Defects Res Part A Clin Mol Teratol. 2009; 88(1) NA – NA. doi: 10.1002/bdra.20621
11. Chen C-P, Huang J-P, Chen Y-Y, et al. Chromosome 22q11.2 deletion syndrome: prenatal diagnosis, array comparative genomic hybridization characterization using uncultured amniocytes and literature review. Gene. 2013; 527(1):405–9. DOI: 10.1016/j.gene.2013.06.009 [PubMed: 23791650]
12. Fishman NH, Hof RB, Rudolph aM, Heymann Ma. Models of congenital heart disease in fetal lambs. Circulation. 1978; 58(2):354–364. DOI: 10.1161/01.CIR.58.2.354 [PubMed: 668085]
13. Hawkins J, Van Hare GF, Schmidt KG, Rudolph AM. Effects of Increasing Afterload on Left Ventricular Output in Fetal Lambs. Circ Res. 1989; 65(1):127–34. [PubMed: 2736730]
14. Lucitti JL, Visconti R, Novak J, Keller BB. Increased arterial load alters aortic structural and functional properties during embryogenesis. Am J Physiol Heart Circ Physiol. 2006; 291(4):H1919–H1926. DOI: 10.1152/ajpheart.01061.2005 [PubMed: 16648183]
15. Hove JR, Köster RW, Forouhar AS, Acevedo-Bolton G, Fraser SE, Gharib M. Intracardiac fluid forces are an essential epigenetic factor for embryonic cardiogenesis. Nature. 2003; 421(6919): 172–177. DOI: 10.1038/nature01282 [PubMed: 12520305]
16. Reckova M, Rosengarten C, deAlmeida A, et al. Hemodynamics is a key epigenetic factor in development of the cardiac conduction system. Circ Res. 2003; 93(1):77–85. DOI: 10.1161/01.RES.0000079488.91342.B7 [PubMed: 12775585]
17. Groenendijk BCW, Van der Heiden K, Hierck BP, Poelmann RE. The role of shear stress on ET-1, KLF2, and NOS-3 expression in the developing cardiovascular system of chicken embryos in a venous ligation model. Physiology (Bethesda). 2007; 22:380–389. DOI: 10.1152/physiol.00023.2007 [PubMed: 18073411]
18. Hogers B, DeRuiter MC, Gittenberger-de Groot aC, Poelmann RE. Extraembryonic venous obstructions lead to cardiovascular malformations and can be embryolethal. Cardiovasc Res. 1999; 41(1):87–99. S0008-6363(98)00218-1 [pii]. [PubMed: 10325956]
19. Vermot J, Forouhar AS, Liebling M, et al. Reversing Blood Flows Act through klf2a to Ensure Normal Valvulogenesis in the Developing Heart. PLoS Biol. 2009; 7(11):e1000246.doi: 10.1371/journal.pbio.1000246 [PubMed: 19924233]
20. Tai L, Zheng Q, Pan S, Jin Z-G, Berk BC. Flow Activates ERK1/2 and Endothelial Nitric Oxide Synthase via a Pathway Involving PECAM1, SHP2, and Tie2. J Biol Chem. 2005; 280(33):29620–29624. DOI: 10.1074/jbc.M501243200 [PubMed: 15985432]
21. Yashiro K, Shiratori H, Hamada H. Haemodynamics determined by a genetic programme govern asymmetric development of the aortic arch. Nature. 2007 Nov.450:1–3. DOI: 10.1038/nature06254
22. Lee TC, Zhao YD, Courtman DW, Stewart DJ. Abnormal Aortic Valve Development in Mice Lacking Endothelial Nitric Oxide Synthase. Circulation. 2000; 101(20):2345–2348. DOI: 10.1161/01.CIR.101.20.2345 [PubMed: 10821808]

23. Jenkins MW, Watanabe M, Rollins AM. Longitudinal Imaging of Heart Development With Optical Coherence Tomography. IEEE J Sel Top Quantum Electron. 2012; 18(3):1166–1175. DOI: 10.1109/JSTQE.2011.2166060 [PubMed: 26236147]
24. Menon V, Eberth J, Goodwin R, Potts J. Altered Hemodynamics in the Embryonic Heart Affects Outflow Valve Development. J Cardiovasc Dev Dis. 2015; 2(2):108–124. DOI: 10.3390/jcdd2020108 [PubMed: 26878022]
25. Johnson B, Bark D, Van Herck I, Garrity D, Dasi LP. Altered mechanical state in the embryonic heart results in time-dependent decreases in cardiac function. Biomech Model Mechanobiol. 2015; 14(6):1379–1389. DOI: 10.1007/s10237-015-0681-1 [PubMed: 25976479]
26. Midgett M, Goenezen S, Rugonyi S. Blood flow dynamics reflect degree of outflow tract banding in Hamburger – Hamilton stage 18 chicken embryos. J R Soc Interface. 2014; 11:20140643. [PubMed: 25165602]
27. Chivukula VK, Goenezen S, Liu A, Rugonyi S. Effect of Outflow Tract Banding on Embryonic Cardiac Hemodynamics. J Cardiovasc Dev Dis. 2016; 3(1)doi: 10.3390/jcdd3010001
28. Hu N, Christensen DA, Agrawal AK, Beaumont C, Clark EB, Hawkins JA. Dependence of Aortic Arch Morphogenesis on Intracardiac Blood Flow in the Left Atrial Ligated Chick Embryo. Anat Rec Adv Integr Anat Evol Biol. 2009; 292(5):652–660. DOI: 10.1002/ar.20885
29. CLARK E, HU N, FROMMELT P, VANDEKIEFT G, DUMMETT J, TOMANEK R. Effect of increased pressure in stage 21 chick embryos on ventricular growth. Am J Physiol. 1989; 257:H55–H61. [PubMed: 2750949]
30. Wells J, Kao C, Jansen ED, Konrad P, Mahadevan-jansen A. Application of infrared light for in vivo neural stimulation. J Biomed Opitics. 2005 Dec 6.10:064003.doi: 10.1117/1.2121772
31. Jenkins MW, Duke AR, Gu S, et al. Optical pacing of the embryonic heart. Nat Photonics. 2010; 4:623–626. DOI: 10.1038/nphoton.2010.166 [PubMed: 21423854]
32. Jenkins MW, Wang YT, Doughman YQ, Watanabe M, Cheng Y, Rollins AM. Optical pacing of the adult rabbit heart. Biomed Opt Express. 2013; 4(9):1626–1635. DOI: 10.1364/BOE.4.001626 [PubMed: 24049683]
33. Wang YT, Gu S, Ma P, Watanabe M, Rollins AM, Jenkins MW. Optical stimulation enables paced electrophysiological studies in embryonic hearts. Biomed Opt Express. 2014; 5(4):1000–1013. DOI: 10.1364/BOE.5.001000 [PubMed: 24761284]
34. Wells J, Kao C, Konrad P, et al. Biophysical Mechanisms of Transient Optical Stimulation of Peripheral Nerve. Biophys J. 2007; 93(7):2567–2580. DOI: 10.1529/biophysj.107.104786 [PubMed: 17526565]
35. Shapiro MG, Homma K, Villarreal S, Richter C-P, Bezanilla F. Infrared light excites cells by changing their electrical capacitance. Nat Commun. 2012; 3:736.doi: 10.1038/ncomms1742 [PubMed: 22415827]
36. Dittami GM, Rajguru SM, Lasher RA, Hitchcock RW, Rabbitt RD. Intracellular calcium transients evoked by pulsed infrared radiation in neonatal cardiomyocytes. J Physiol. 2011; 589(Pt 6):1295–1306. DOI: 10.1113/jphysiol.2010.198804 [PubMed: 21242257]
37. Hamburger VHLH. A series of normal stages in the development of the chick embryo. Dev Dyn. 1951; 88(1):49–92. DOI: 10.1002/aja.1001950404
38. Huang D, Swanson EA, Lin CP, et al. Optical coherence tomography. Science. 1991; 254(5035): 1178–1181. [PubMed: 1957169]
39. Peterson LM, Gu S, Jenkins MW, Rollins AM. Orientation-independent rapid pulsatile flow measurement using dual-angle Doppler OCT. Biomed Opt Express. 2014; 5(2):499–514. DOI: 10.1364/BOE.5.000499 [PubMed: 24575344]
40. Peterson LM, Jenkins MW, Gu S, Barwick L, Watanabe M, Rollins AM. 4D shear stress maps of the developing heart using Doppler optical coherence tomography. Biomed Opt Express. 2012; 3(11):3022–3032. DOI: 10.1364/BOE.3.003022 [PubMed: 23162737]
41. Larina IV, Sudheendran N, Ghosn M, et al. Live imaging of blood flow in mammalian embryos using Doppler swept-source optical coherence tomography. J Biomed Opt. 2008; 13(6): 060506.doi: 10.1117/1.3046716 [PubMed: 19123647]
42. Hu Z, Rollins AM. Fourier domain optical coherence tomography with a linear-in-wavenumber spectrometer. Opt Lett. 2007; 32(24):3525.doi: 10.1364/OL.32.003525 [PubMed: 18087530]

43. Kuwajima T, Sitko Aa, Bhansali P, Jurgens C, Guido W, Mason C. ClearT: a detergent- and solvent-free clearing method for neuronal and non-neuronal tissue. Development. 2013; 140(6): 364–1368. DOI: 10.1242/dev.091844
44. Karunamuni G, Gu S, Doughman YQ, et al. Using optical coherence tomography to rapidly phenotype and quantify congenital heart defects associated with prenatal alcohol exposure. Dev Dyn. 2015; 244(4):607–618. DOI: 10.1002/dvdy.24246 [PubMed: 25546089]
45. Heckel E, Boselli F, Roth S, et al. Oscillatory Flow Modulates Mechanosensitive klf2a Expression through trpv4 and trpp2 during. Heart Valve Development. 2015; 25doi: 10.1016/j.cub. 2015.03.038
46. Boselli F, Vermot J. Live imaging and modeling for shear stress quantification in the embryonic zebrafish heart. Methods. 2015; doi: 10.1016/j.ymeth.2015.09.017
47. Steed E, Boselli F, Vermot J. Hemodynamics driven cardiac valve morphogenesis. Biochim Biophys Acta - Mol Cell Res. 2015; doi: 10.1016/j.bbamcr.2015.11.014
48. Karunamuni GH, Ma P, Gu S, Rollins AM, Jenkins MW, Watanabe M. Connecting Teratogen-Induced Congenital Heart Defects to Neural Crest Cells and Their Effect on Cardiac Function.
49. Liu Y, Guo L, Tian Z, et al. A retrospective study of congenital scoliosis and associated cardiac and intraspinal abnormities in a Chinese population. Eur Spine J. 2011; 20(12):2111–2114. DOI: 10.1007/s00586-011-1818-2 [PubMed: 21533853]
50. Sparrow DB, Chapman G, Smith AJ, et al. A mechanism for gene-environment interaction in the etiology of congenital scoliosis. Cell. 2012; 149(2):295–306. DOI: 10.1016/j.cell.2012.02.054 [PubMed: 22484060]
51. Hoffman JI, Kaplan S. The incidence of congenital heart disease. J Am Coll Cardiol. 2002; 39(12): 1890–1900. DOI: 10.1016/S0735-1097(02)01886-7 [PubMed: 12084585]
52. Lloyd-Jones D, Adams RJ, Brown TM, et al. Executive Summary: Heart Disease and Stroke Statistics--2010 Update: A Report From the American Heart Association. Circulation. 2010; 121(7):948–954. DOI: 10.1161/CIRCULATIONAHA.109.192666 [PubMed: 20177011]
53. van der Linde D, Konings EEM, Slager MA, et al. Birth Prevalence of Congenital Heart Disease Worldwide: A Systematic Review and Meta-Analysis. J Am Coll Cardiol. 2011; 58(21):2241–2247. DOI: 10.1016/J.JACC.2011.08.025 [PubMed: 22078432]
54. Ferencz C, Boughman JA, Neill CA, Brenner JI, Perry LW. Group TB-WIS. Congenital cardiovascular malformations: Questions on inheritance. J Am Coll Cardiol. 1989; 14(3):756–763. DOI: 10.1016/0735-1097(89)90122-8 [PubMed: 2768723]
55. Pierpont ME, Basson CT, Benson DW, et al. Genetic Basis for Congenital Heart Defects: Current Knowledge: A Scientific Statement From the American Heart Association Congenital Cardiac Defects Committee, Council on Cardiovascular Disease in the Young: Endorsed by the American Academy of Pediatrics. Circulation. 2007; 115(23):3015–3038. DOI: 10.1161/CIRCULATIONAHA.106.183056 [PubMed: 17519398]
56. Goenezen S, Chivukula VK, Midgett M, Phan L, Rugonyi S. 4D subject-specific inverse modeling of the chick embryonic heart outflow tract hemodynamics. Biomech Model Mechanobiol. 15(3): 723–743. DOI: 10.1007/S10237-015-0720-Y

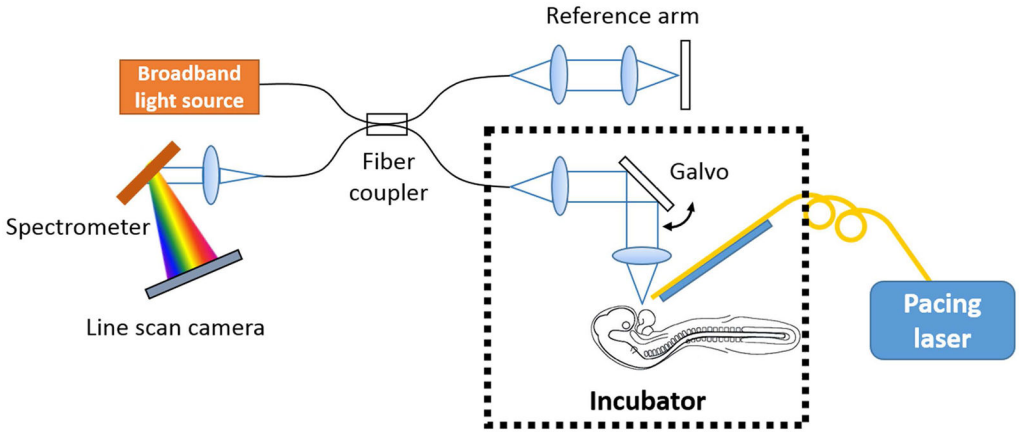

Figure 1.

OP/OCT setup for pacing and imaging quail embryos. The system is housed within an incubator to ensure physiologic development of the embryos.

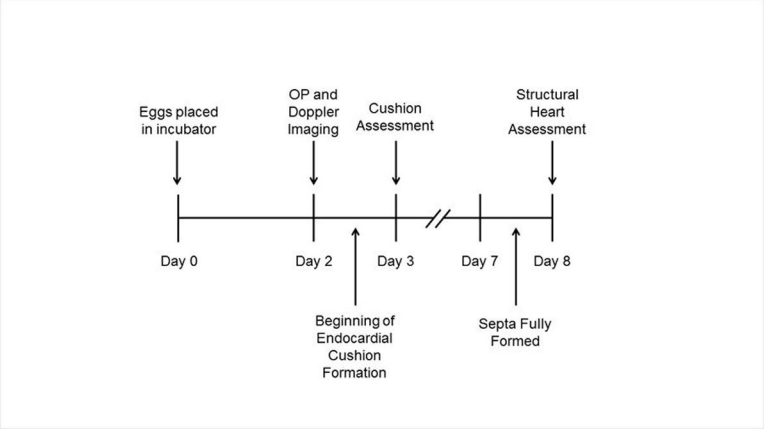

Figure 2.
Timeline of experiments

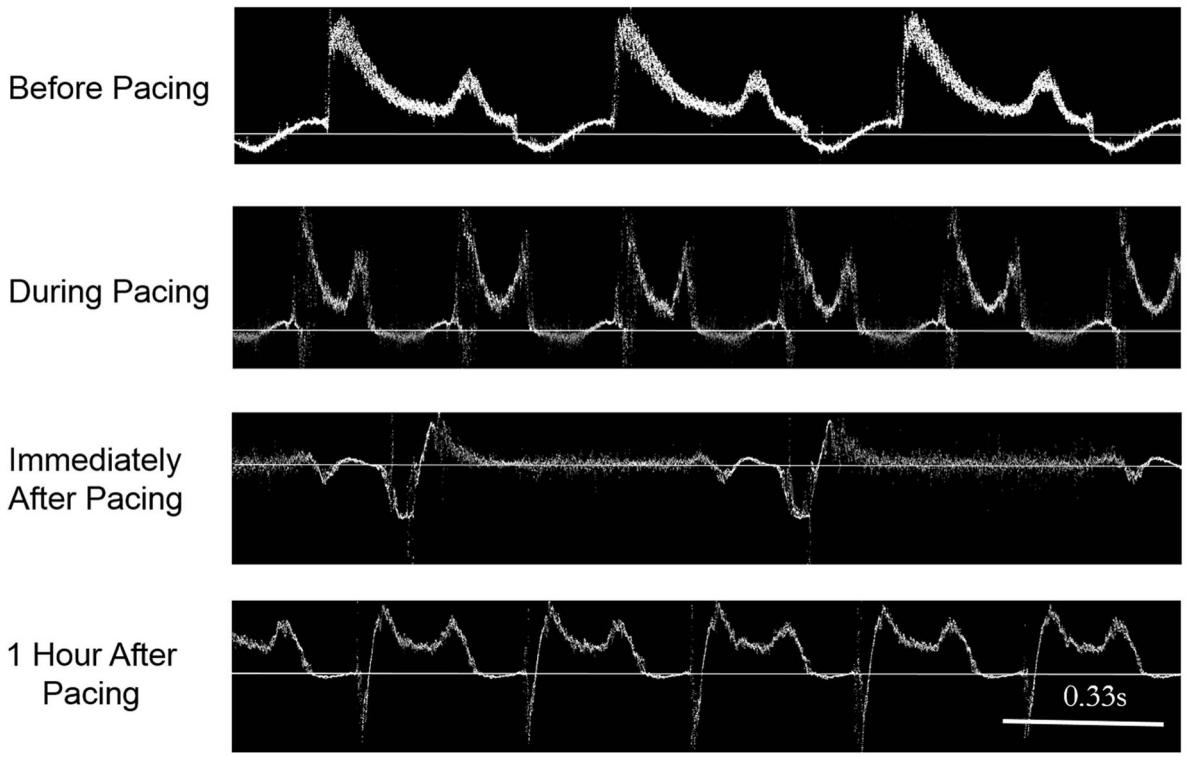

Figure 3.

Pulsed Doppler OCT tracings from the inflow tract of the 2-day (stage 14) embryonic quail heart before, during, immediately after, and 1 hour after optical pacing (OP). Deflection above the solid line indicates forward flow, while deflection below denotes regurgitant flow.

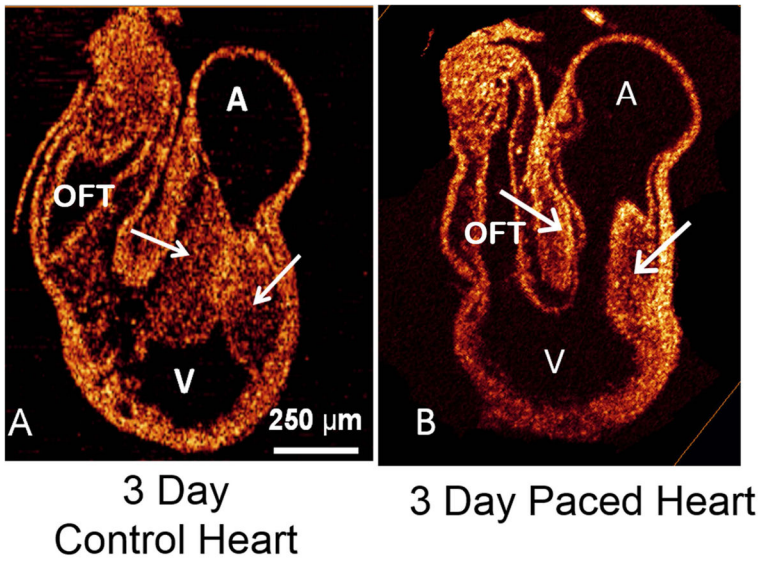

Figure 4.

2-D OCT slices of control (A) and paced (B) 3-day (stage 19) quail hearts. The control heart maintains a normal phenotype, while the paced has abnormal formation and alignment of the cushions and tube. A – Atria, V – Ventricle, OFT – Out Flow Tract. Arrows indicate endocardial cushions

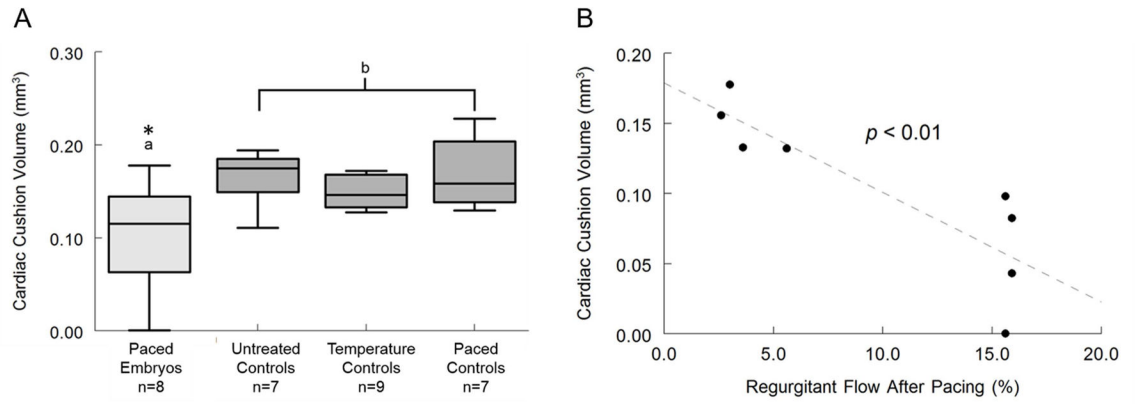

Figure 5.

(A) Volumes of cardiac cushions in control and paced embryos, which are inversely correlated with regurgitant flow fraction. (B) The regurgitant flow fraction in the embryo immediately after pacing on day 2 is inversely correlated with the volume of endocardial cushions on day 3.

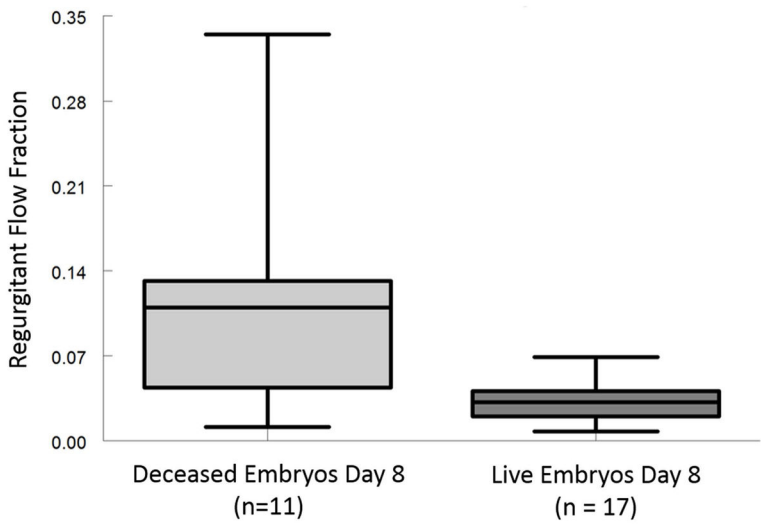

Figure 6.

Embryos with greatly increased regurgitant flow fraction on day 2 after pacing tended to die by day 8. These embryos also had smaller cardiac cushions, which suggests that the most severely affected endocardial cushion are lethal.

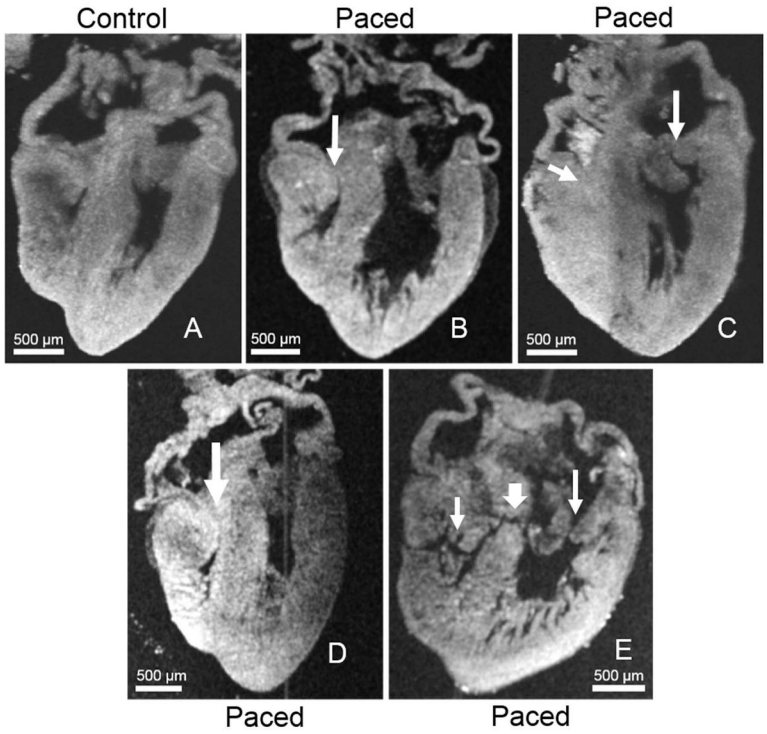

Figure 7.

Examples of pacing-induced CHDs. A Control 8 day heart. B Paced heart with tricuspid atresia, indicated by arrow. C Paced heart with tricuspid atresia (small arrow), severely hypoplastic right ventricle with hypertrophy, dysplastic mitral valve (large arrow). D Paced heart with dilated, thin-walled, and hypoplastic right ventricle, and an Ebsteinoid tricuspid valve (arrow). E Paced heart with a common atrioventricular canal, with tricuspid valve (small arrow), mitral valve (long arrow), and atrioventricular septal defect (fat arrow) at the same level.

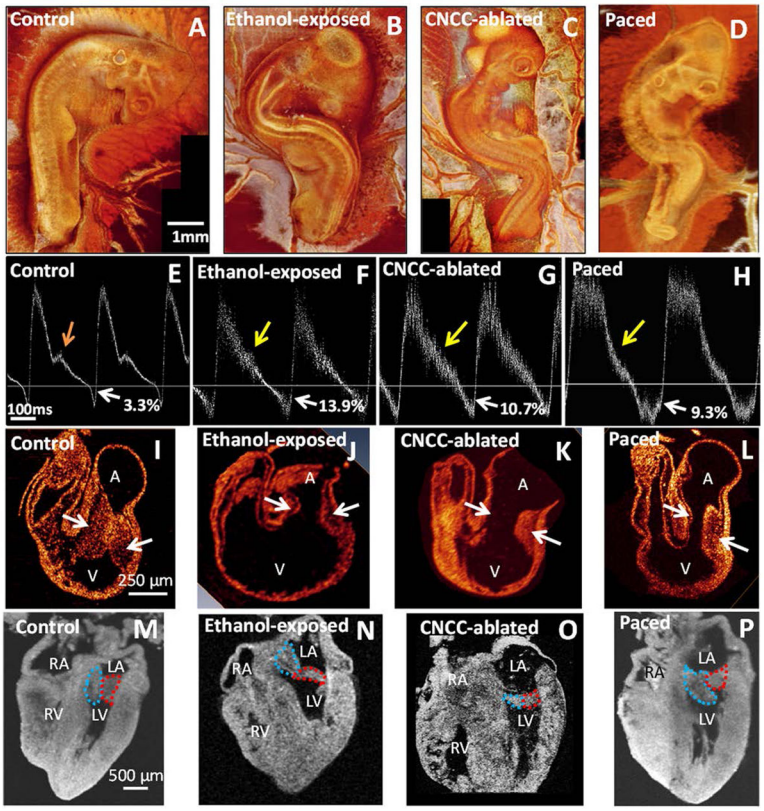

Figure 8.

Comparison of pacing-induced cardiac defects with fetal alcohol syndrome (ethanol exposed) and velo-cardio-facial syndrome/Digeorge (cardiac neural crest cell (CNCC) ablation) models. A–D are representative day 3 3-D OCT reconstructions. The control embryo (A) displays normal cranial and cervical flexures and a relatively straight trunk. Ethanol-exposed (B), CNCC-ablated (C), and paced (D) embryos lack proper cranial and cervical flexures and exhibit an S-shape twist of the whole body, which may be the beginning signs of scoliosis, a comorbidity of CHDs. E–H are representative day 3 pulsed-Doppler traces. The horizontal line delineates forward (above) and regurgitant (below) flows. Control embryos (E) always have a notch indicated by the orange arrow and mild regurgitation (white arrow, 1–3%). Pulsed-Doppler waveforms from the ethanol-exposed (F), CNCC-ablated (G) and paced (H) embryos often have reduced or absent shoulders (yellow arrows) and significantly increased retrograde flow (white arrows). I-L show day 3 cross sections of the heart, with the atrioventricular (AV) cushions (valve precursors) separating the primitive atrium and ventricle (white arrows). The control heart (I) displays large AV cushions, while those of the ethanol-exposed (J), CNCC-ablated (K) and paced (L) hearts are distorted and much smaller. M-P show the resultant heart morphology at day 8, with mitral leaflets outlined in red and blue. Valves are thicker at this stage of development than at maturity. The ethanol-exposed (M), CNCC-ablated (N), and paced (O) hearts show unusual morphology and coaptation of the leaflets. The paced heart (P) demonstrates severe right ventricular hypoplasia, tricuspid atresia, and a malformed mitral valve. We believe altered hemodynamics is a contributing factor in all three models and explains the similar

phenotypes. Altered hemodynamics leads to smaller cardiac cushions, which develop into abnormally shaped valve leaflets. A – atrial region; V – ventricular region; LA – left atrium; RA – right atrium; LV left ventricle; RV – right ventricle

Table 1

Day 8 Congenital Heart Defects	Number of Hearts Affected
Valve Defects (e.g. atresia, stenosis, hypoplasia, dysplasia, hypoplasia)	8/18 (44.4%)
Ventricular Septal Defects	3/18 (16.7%)
Hypoplastic Right Ventricle	7/18 (38.9%)
Septal Hypertrophy	5/18 (27.8%)
Common Atrioventricular Canal	2/18 (11.1%)
Ebstein's Anomaly or Ebsteinoid Dysplasia	2/18 (11.1%)
No Defect	1/18 (5.6%)